



# Research on the effect of hydrogen charging on the extreme tip bending performance of ultra high strength automotive steel plate

Jian Wang<sup>1,2</sup>, Hongzhou Lu<sup>3,a</sup>, Xiangxing Deng<sup>1</sup>, Lintao Gui<sup>1</sup>, Aimin Guo<sup>3</sup>,  
Feng Yang<sup>4</sup> and Yan Zhao<sup>1,b,\*</sup>

<sup>1</sup>*Equipment Lightweight Technology Institute, Beijing Institute of Technology Chongqing Innovation Center, Chong Qing, 401120, China*

<sup>2</sup>*College of Materials Science and Engineering, Chongqing University, Chong Qing, 400045, China*

<sup>3</sup>*CITIC Metal Co., Ltd. Beijing, 100004, China*

<sup>4</sup>*Technology Center of Tangshan Iron and Steel Group Co., Ltd. Tangshan, 063016, China*  
Email: <sup>a</sup>luhz@citic.com, <sup>b,\*</sup>yan.zhao11@icloud.com

In this study, the effect of hydrogen charging treatment on the extreme tip bending performance of ultra-high strength automotive steel plates was investigated. After electrochemical hydrogenation, the extreme tip bending angle of the steel plate decreased to varying degrees, and the downward trend began to converge after 6 hours of hydrogenation. After 6 hours of hydrogen charging, the extreme tip bending angle of 22MnB5 bare plate decreased by 49.2%, 22MnB5-NbV by 36.7%, 34MnB5 by 49%, 34MnB5-V by 34.6%, and 34MnB5-Nb by 30.8% respectively. In addition, Al-Si coated plates need to be pre-bended treatment before the experiment to produce micro cracks on the surface to get the chance of the hydrogen getting into the plate. The influence of hydrogen overflow on the extreme tip bending angle was also studied, and it was found that the filled hydrogen will overflow completely after 24 hours. Therefore, this report summarizes the effect of hydrogen content on the extreme tip bending angle, hoping to provide positive guidance for future research on the hydrogen embrittlement resistance of high-strength steels.

*Keywords:* Hydrogen charging; Extreme tip bending; Hydrogen embrittlement.

## 1. Introduction

With the upgrading of the global automotive industry and the comprehensive rise of manufacturing and marketing of China's new energy vehicles, the steels used in automobiles are gradually shifting towards high strength and elongation. The application volume of high-strength steels (USS), advanced high-strength steels (AHSS), or ultra-high-strength steels (UHSS) have been becoming increasingly widespread. It is well known that hydrogen embrittlement behavior occurs when the strength of steels exceeds 1000MPa, which has always affected the research and development of UHSS of 1500MPa and above<sup>[1-4]</sup>. How to enhance the hydrogen embrittlement resistance of HSS, and objectively

---

\*The work is financially supported by the Project of Development of 1.8-2.0GPa high toughness PHS from CITIC Group (Grant No 2022FWNB-30055), Major Scientific and Technological Innovation Project of CITIC Group (Grant No. 2022zxkya06100), China Postdoctoral Science Foundation (Grant No. 2022M710399), Chongqing Post doctoral Science Foundation (Grant No. cstc2021jcyj-bshX0003), Chongqing Talent Plan (Grant No. CQYC20210301387).

© The Author(s) 2024

Y. Zhang and M. Ma (eds.), *Proceedings of the 7th International Conference on Advanced High Strength Steel and Press Hardening (ICHSSU 2024)*, Atlantis Highlights in Materials Science and Technology 3,  
[https://doi.org/10.2991/978-94-6463-581-2\\_35](https://doi.org/10.2991/978-94-6463-581-2_35)

and rapidly evaluate its effect degree, occurring mechanism and accident time, are the hottest topics of considerable concerns of the vehicle safety among domestic and international scholars [5-9]. The extreme tip bending test is an important parameter for quickly evaluating toughness and the minimum bending angle at which automotive steel plates will fracture, which is crucial for the automotive industry. If the extreme tip bending performance can be used to evaluate the hydrogen embrittlement resistance, it will greatly improve the efficiency and accuracy of evaluating the hydrogen embrittlement resistance. Therefore, the author conducted hydrogen charging at different current and time, and studied the effect of hydrogen charging treatment on the extreme tip bending performance of UHSS from a macroscopic perspective.

## 2. Experimental Materials and Methods

### 2.1. Experimental Steels and Treatment

The UHSS used were all PHS (Press Hardened Steel), including 2 types of uncoated 22MnB5 steel plates, 3 types of uncoated 34MnB5 steel plates, and one type of 22MnB5-AlSi steel plate. The thickness of both 22MnB5 and 34MnB5 steel plates was 1.5 mm, and the thickness of 22MnB5-AlSi steel plate was 1.0 mm. The chemical composition is shown in Table 1.

Table 1 The chemical compositions of the studied steels (in wt%)

Steel	C	Si	Mn	Al	Cr	B	Ti	Nb	V
22MnB5-1	0.22	0.24	1.30	0.03	0.13	0.002	0.031	0	0
22MnB5-2	0.23	0.23	1.32	0.03	0.14	0.002	0.033	0.04	0.04
34MnB5-1	0.33	0.31	1.45	0.03	0.55	0.002	0.030	0	0
34MnB5-2	0.34	0.31	1.50	0.03	0.59	0.002	0.035	0	0.20
34MnB5-3	0.34	0.64	1.28	0.03	0.60	0.002	0.028	0.08	0
22MnB5-AlSi	0.22	0.24	1.30	0.03	0.13	0.002	0.031	0	0

The steel plates were heated at 930 °C, and held for 5 minutes for austenitization [10]. Then quenched by mold pressing to room temperature, and the microstructure after quenched was all martensite. The tensile strength of 22MnB5 is about 1500MPa, and the tensile strength of 34MnB5 is about 1900MPa. Cut the quenched plate into standard specimen size which was 60 mm at rolling direction and 30 mm at perpendicular rolling direction. Then, polish its surface in sequence with 180-1200 mesh SiC sandpaper until the surface is smooth and free of oxide skin.

The polished samples of uncoated 22MnB5 and 34MnB5 steel plates were subjected to hydrogen charging treatment. The hydrogen charging solution was NaOH with a concentration of 1mol/L, and 1g/L of CH<sub>4</sub>N<sub>2</sub>S alkaline aqueous solution was added. The hydrogen charging current was 20mA/cm<sup>2</sup>, and the hydrogen charging time was 0.5-24 hours. The steel type to be tested was the cathode, and the carbon rod was the anode. In

addition, the 22MnB5-AlSi steel plate needs to be pre bent before hydrogen charging treatment.

After hydrogen charging of the sample steel, the extreme tip bending test shall be carried out immediately, and the test execution standard is T/CSAE 154-2020 “Ultra high strength automobile steel plate-Extreme tip bending test”.

This paper introduces the sensitivity coefficient  $I_d$  of extreme tip bending, and its calculation formula is shown in Equation (1),

$$I_d = 100\% \times (D_s - D_f)/D_s \tag{1}$$

Where  $D_s$  is the extreme tip bending without hydrogen charging, and  $D_f$  is the extreme tip bending after 6 hours of hydrogen charging. The smaller the sensitivity coefficient  $I_d$  of extreme tip bending, the better the hydrogen embrittlement resistance.

**2.2. Experimental equipment**

The hydrogen charging power supply is a domestically produced equipment, model UNI-T-UPT1310, with an output current of 20mA/cm<sup>2</sup>.

The testing equipment for extreme tip bending performance is a universal tensile testing machine with an extreme tip bending fixture, and the testing principle diagram is shown in Figure 1. The brand and model of the universal stretching machine is Zwick/Roell-Z100, with a maximum range of 100kN and a set pressing speed of 15mm/min.

The thermal desorption spectroscopy (TDS) equipment consists of a vacuum pumping system, glass tube, heating furnace, and quadrupole mass spectrometer (INFICON, USA). During testing, the vacuum pressure is below 1.2×10<sup>-4</sup>Pa, with a heating rate of approximately 10K/min, and a maximum testing temperature of 800°C. A quadrupole mass spectrometer is used to measure the hydrogen content absorbed from the sample during the desorption process. Measure the hydrogen content absorbed from the sample during the temperature ramp-up process using a quadrupole mass spectrometer.

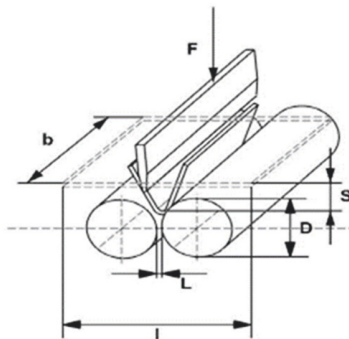


Figure 1. The principle of extreme tip bending test

In Figure 1, F is the bending load, S is the punch displacement, D is the roller diameter, L is the roller distance, l is the sample length, b is the sample width.

### 2.3. Experimental Plan

Three experimental plans were designed as following:

Plan 1, Hydrogen charging → Extreme tip bending test. 22MnB5-1, 22MnB5-2, 34MnB5-1, 34MnB5-2 were hydrogen charged for 0.5h, 1h, 3h, 6h, 12h, and 24h, respectively, with a hydrogen charging current of 20mA/cm<sup>2</sup>. Immediately after hydrogen charging, conducted the extreme tip bending test to obtain the relationship between hydrogen charging time and the extreme tip bending angle.

Plan 2, Pre bending → Hydrogen charging → Extreme tip bending test. The 22MnB5-AlSi steel plate was pre bent at 20° to produce micro cracks on the surface, and then subjected to hydrogen charging treatment for 5min, 10min, 20min, 60min, and 120min, with a hydrogen charging current of 10mA/cm<sup>2</sup>. Immediately after hydrogen charging, conducted the extreme tip bending test to obtain the relationship between hydrogen charging time and the extreme tip bending angle.

Plan 3, Pre bending → Hydrogen charging → Placement → Extreme tip bending test. The 22MnB5-AlSi steel plate was pre bent at 20° to produce micro cracks on the surface, and then subjected to 20 minutes of hydrogen charging treatment with a hydrogen charging current of 10mA/cm<sup>2</sup>. Then, it was placed for 3h, 6h, 15h, 24h, 48h, 72h, and 96h respectively. The specimen was further subjected to extreme tip bending test to obtain the relationship between the placement time and the extreme tip bending angle.

## 3. Result and discussion

### 3.1. Hydrogen charging → Extreme tip bending test

According to the plan 1, extreme tip bending test were conducted after hydrogen charging, with a hydrogen charging current of 20mA/cm<sup>2</sup>. The results are shown in Table 2 and Figure 2 and 3. According to the results, the longer the hydrogen charging time, the smaller the extreme tip bending angle gradually decreases, and the extreme tip bending angle tends to stabilize after 6 hours of hydrogen charging. Due to the effective enhancement of hydrogen embrittlement resistance by elements Nb and V [10-14], the extreme tip bending angle of 22MnB5-2 after hydrogen charged was higher than the 22MnB5-1, and the 34MnB5-2 and 34MnB5-3 were higher than the 34MnB5-1. After 6 hours of hydrogen charging, the extreme tip bending sensitivity coefficients of 22MnB5-1 and 22MnB5-2 were 49.2% and 36.7%, respectively, and the extreme tip bending sensitivity coefficients of 1900-1, 1900-2, and 1900-3 were 49.0%, 34.6%, and 30.8%, respectively. The smaller the extreme tip bending sensitivity coefficient  $I_d$ , the better the hydrogen embrittlement resistance. Therefore, the  $I_d$  value of PHS with excellent resistance to hydrogen embrittlement is lower than that of ordinary PHS.

In order to evaluate the hydrogenation effect, samples of 34MnB5-1 were selected and subjected to TDS test to measure the hydrogen content after 1 hour and 6 hours of hydrogenation, as shown in Figure 4 and Figure 5. The results indicate that the hydrogen content is approximately 11 ppm after 1 hour of hydrogenation, and approximately 32 ppm after 6 hours.

Table 2 Results of extreme tip bending test after hydrogen charging

Charging time (h)	Extreme tip bending angle (deg)				
	22MnB5-1	22MnB5-2	34MnB5-1	34MnB5-2	34MnB5-3
No charging	59	60	51	52	52
0.5	48	50	42	48	50
1	44	46	38	43	44
3	36	40	32	38	40
6	30	38	26	34	36
12	29	37	25	32	35
24	29	37	25	32	35
$I_d$	49.2%	36.7%	49.0%	34.6%	30.8%

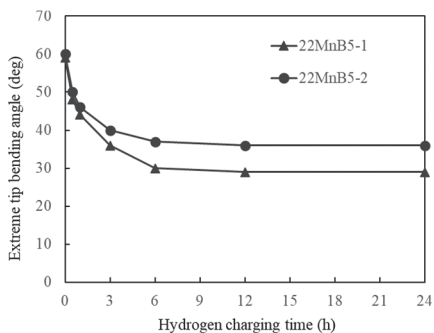


Figure 2 The relationship between 22MnB5 hydrogen charging time and extreme tip bending angle

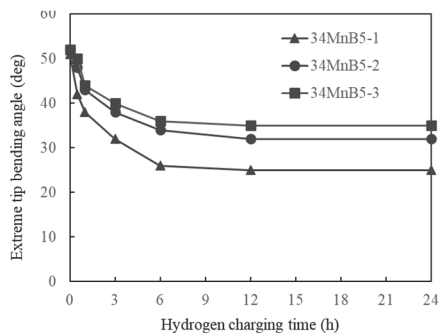


Figure 3 The relationship between 34MnB5 hydrogen charging time and extreme tip bending angle

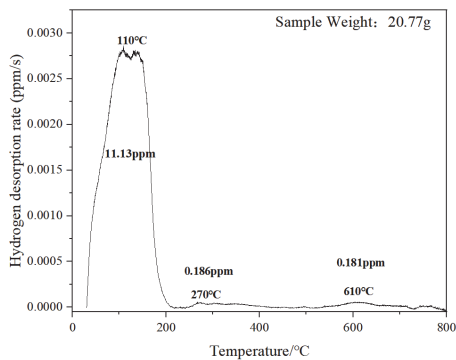


Figure 4 TDS test results of 34MnB5-1 sample after hydrogen charging for 1 hour

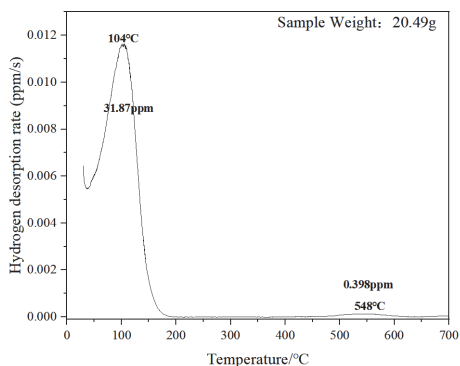


Figure 5 TDS test results of 34MnB5-1 sample after hydrogen charging for 6 hours

**3.2. Pre bending → Hydrogen charging → Extreme tip bending test**

According to Plan 2, a pre-bending of 20° was performed on the 22MnB5-AlSi sheet to induce microcracks on the surface of the material, as shown in Figure 6. The pre bending sample were subjected to the extreme tip bending test after hydrogen charging, with a hydrogen charging current of 10mA/cm<sup>2</sup>. The results of the test are shown in Figure 7.

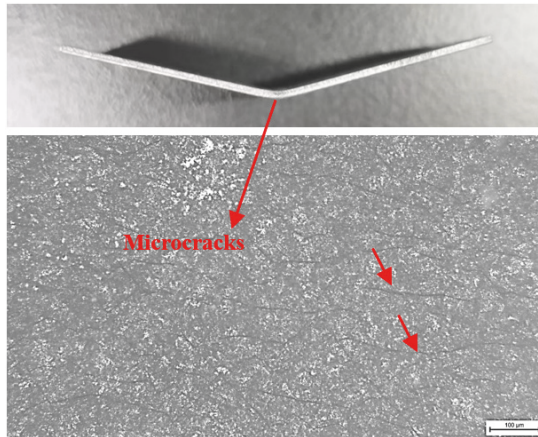


Figure 6 Surface microcracks after pre bending

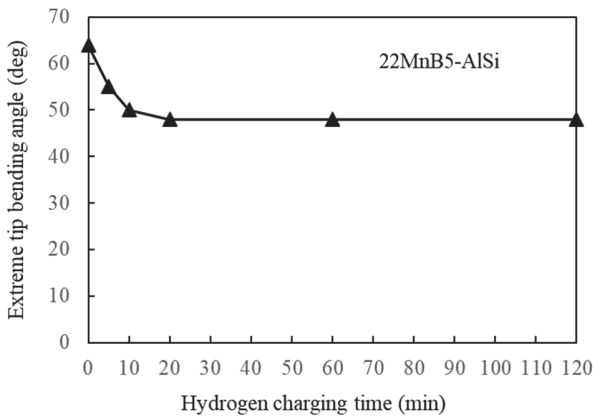


Figure 7 The relationship between hydrogen charging time and extreme tip bending angle of 22MnB5-AlSi Plate

**3.3. Pre bending → Hydrogen charging → Placement → Extreme tip bending test**

According to Plan 3, a pre-bending of 20° was performed on the 22MnB5-AlSi plate to induce microcracks on the surface of the material. The sample was then hydrogen charged for 20 minutes until it reached a state of full or over-saturation with hydrogen, before being left for up to a maximum of 96 hours prior to conducting the extreme tip bending test. The results of the test are shown in Figure 8. From the results, it can be observed that within 6 hours of hydrogenation, there is no significant change in the angle of the extreme tip

bending, indicating an over-saturation state of hydrogenation previously. Furthermore, after 24 hours of placement, the angle tends to stabilize and return to the state without hydrogenation, indicating that all hydrogen has diffused out after 24 hours.

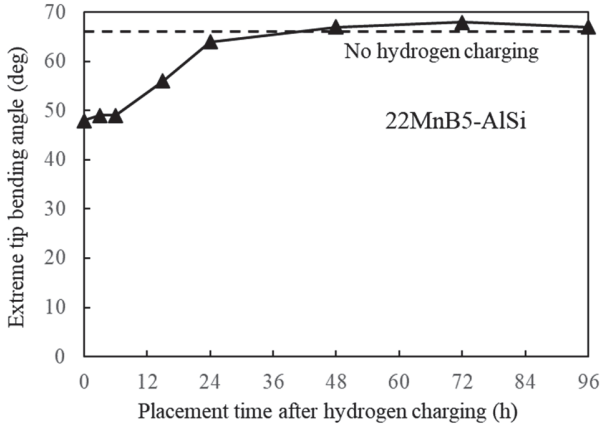


Figure 8 The relationship between the placement time of 22MnB5-AlSi plate after hydrogen charging and the extreme tip bending angle

#### 4. Conclusion

(1) As the hydrogen charging time increases, the extreme tip bending angle gradually decreased. The uncoated 22MnB5 and 34MnB5 steel plates would converge after 6 hours of hydrogen charging at a hydrogen charging current of  $20\text{mA}/\text{cm}^2$ , indicating that hydrogen charging was beginning to saturate. After 6 hours of hydrogen charging, the extreme tip bending sensitivity coefficients ( $I_d$ ) of 22MnB5-1 and 22MnB5-2 were 49.2% and 36.7%, respectively. The extreme tip bending sensitivity coefficients of 1900-1, 1900-2, and 1900-3 were 49.0%, 34.6%, and 30.8%, respectively. It can be seen that the  $I_d$  value of PHS with excellent resistance to hydrogen embrittlement is lower than that of ordinary PHS. Therefore, using this method can easily and quickly evaluate the hydrogen embrittlement resistance of ultra-high strength steel plates.

(2) After the appearance of microcracks on the surface of 22MnB5-AlSi steel plate, with the hydrogen charging current of  $10\text{mA}/\text{cm}^2$ , under 20 minutes of hydrogen charging, the extreme tip bending angle will be converged, indicating that the surface would accelerate saturation after microcracks.

(3) After 24 hours of placement following hydrogenation, the angle of the extreme tip bending returned to the value of the non-hydrogenated state, indicating that all hydrogen introduced during hydrogenation had been completely eliminated.

The significance of this paper is to study the effect of hydrogen on the performance of ultra-high strength steel plates by changing the extreme tip bending angle through hydrogen charging and hydrogen emission, providing new ideas for evaluating the toughness and hydrogen embrittlement resistance of ultra-high strength steel plates.

## References

1. Lovicu G, Bottazzi M, Aiuto F D, et al. Hydrogen embrittlement of automotive advanced high-strength steels. *Metallurgical and Materials Transactions A*, 2012, 43(11): 4075-4087.
2. Loidl M, Kolk O, Veith S, Goebel T. Characterization of hydrogen embrittlement in automotive advanced high strength steels. *MATERIALWISSENSCHAFT UND WERKSTOFFTECHNIK*. 2011.42, 12, 1105-1110.
3. L. Lin, B.S. Li, G.M. Zhu, Y.L. Kang, R.D. Liu. Effect of niobium precipitation behavior on microstructure and hydrogen induced cracking of press hardening steel 22MnB5. *Materials Science Engineering. A-Struct.* 721 (2018) 38–46.
4. Y. Chen, Z.M. Xu, X.X. Zhang, T.Y. Zhang, J.J. Tang, Z.Q. Sun, Y.F. Sui, X.H. Han, Irreversible hydrogen embrittlement study of B1500HS high strength boron steel. *Materials and Design*. 199(2021).
5. Lawrence Cho, Dimas H. Sulistiyo, Eun Jung Seo, et al. Hydrogen absorption and embrittlement of ultra-high strength aluminized press hardening steel. *Materials Science & Engineering A* 734 (2018) 416–426.
6. Hardy M, Takehide S. Alloy Optimization for Reducing Delayed Fracture Sensitivity of 2000 MPa Press Hardening Steel. *Metals* 2020, 10, 853.
7. Lin Y, Yi H, et al. Role of Vanadium Carbide in Hydrogen Embrittlement of Press-Hardened Steels: Strategy From 1500 to 2000 MPa. *Frontiers in materials*. 2021.7 611390.
8. Shusaku Takagi, Yuki Toji, et al. Hydrogen Embrittlement Resistance Evaluation of Ultra High Strength Steel Sheets for Automobiles. *ISIJ International*, Vol.52 (2012), No.2, pp.316–322.
9. Xinfeng Li, Xianfeng Ma, Jin Zhang, et al. Review of Hydrogen Embrittlement in Metals: Hydrogen Diffusion, Hydrogen Characterization, Hydrogen Embrittlement Mechanism and Prevention. *Acta Metallurgica Sinic (English letters)*. 2020. Vol.33(6): 759-773.
10. GU L M, WEI Y F, YE Y. Research on Hydrogen Embrittlement Sensitivity of 1800 MPa Hot Forming Steel. *Automobile Technology & Material*,2022(6):59-62.
11. Lintao Gui, Yan Zhao, Yi Feng, Mingtu Ma, Hongzhou Lu, et al. Study on the improving effect of Nb-V microalloying on the hydrogen induced delayed fracture property of 22MnB5 press hardened steel. *Materials & Design* 227 (2023) 111763.
12. Weijian Chen, Weiyang Zhao, Pengfei Gao, Feng Li et al. Interaction between dislocations, precipitates and hydrogen atoms in a 2000 MPa grade hot-stamped steel. *Journal of material sresearch and technology* 2022; 18: 4353-4366.
13. Jisung Yoo, Min Chul Jo, Jian Bian, et al. Effects of Nb or (Nb + Mo) alloying on Charpy impact, bending, and delayed fracture properties in 1.9-GPa-grade press hardening steels. *Materials Characterization* 176 (2021) 111133.
14. Huibin Wu, Biao Ju, Di Tang, et al. Effect of Nb addition on the microstructure and mechanical properties of an 1800 MPa ultrahigh strength steel. *Materials Science & Engineering A* 622 (2015) 61-66.



**Open Access** This chapter is licensed under the terms of the Creative Commons Attribution-NonCommercial 4.0 International License (<http://creativecommons.org/licenses/by-nc/4.0/>), which permits any noncommercial use, sharing, adaptation, distribution and reproduction in any medium or format, as long as you give appropriate credit to the original author(s) and the source, provide a link to the Creative Commons license and indicate if changes were made.

The images or other third party material in this chapter are included in the chapter's Creative Commons license, unless indicated otherwise in a credit line to the material. If material is not included in the chapter's Creative Commons license and your intended use is not permitted by statutory regulation or exceeds the permitted use, you will need to obtain permission directly from the copyright holder.

